

# Radiation-induced functional connectivity alterations in nasopharyngeal carcinoma patients with radiotherapy

Qiongmin Ma, MD<sup>a</sup>, Donglin Wu, MD<sup>b</sup>, Ling-Li Zeng, PhD<sup>a</sup>, Hui Shen, PhD<sup>a</sup>, Dewen Hu, PhD<sup>a,\*</sup>, Shijun Qiu, PhD<sup>b,\*</sup>

## Abstract

The study aims to investigate the radiation-induced brain functional alterations in nasopharyngeal carcinoma (NPC) patients who received radiotherapy (RT) using functional magnetic resonance imaging (fMRI) and statistic scale.

The fMRI data of 35 NPC patients with RT and 24 demographically matched untreated NPC patients were acquired. Montreal Cognitive Assessment (MoCA) was also measured to evaluate their global cognition performance. Multivariate pattern analysis was performed to find the significantly altered functional connections between these 2 groups, while the linear correlation level was detected between the altered functional connections and the MoCA scores.

Forty-five notably altered functional connections were found, which were mainly located between 3 brain networks, the cerebellum, sensorimotor, and cingulo-opercular. With strictly false discovery rate correction, 5 altered functional connections were shown to have significant linear correlations with the MoCA scores, that is, the connections between the vermis and hippocampus, cerebellum lobule VI and dorsolateral prefrontal cortex, precuneus and dorsal frontal cortex, cuneus and middle occipital lobe, and insula and cuneus. Besides, the connectivity between the vermis and hippocampus was also significantly correlated with the attention score, 1 of the 7 subscores of the MoCA.

The present study provides new insights into the radiation-induced functional connectivity impairments in NPC patients. The results showed that the RT may induce the cognitive impairments, especially the attention alterations. The 45 altered functional connections, especially the 5 altered functional connections that were significantly correlated to the MoCA scores, may serve as the potential biomarkers of the RT-induced brain functional impairments and provide valuable targets for further functional recovery treatment.

**Abbreviations:** ADHD = attention deficit hyperactivity disorder, CTV = clinic target volume, dFC = dorsal frontal cortex, dlPFC = dorsolateral prefrontal cortex, FDR = false discovery rate, FLAIR = fluid-attenuated inversion recovery, fMRI = functional magnetic resonance imaging, GTV = gross tumor volume, IMRT = intensity-modulated radiation therapy, KPS = Karnofsky performance status, LLE = locally linear embedding, LOOCV = leave-one-out cross-validation, MNI = Montreal Neurological Institute, MoCA = Montreal Cognitive Assessment, MVPA = multivariate pattern analysis, NPC = nasopharyngeal carcinoma, RT- = patients not receiving radiotherapy, RT = radiotherapy, RT+ = patients receiving radiotherapy, SVM = support vector machine.

**Keywords:** cognition, functional magnetic resonance imaging, multivariate pattern analysis, nasopharyngeal carcinoma, radiotherapy

Editor: Heye Zhang.

QM and DW have contributed equally to this work.

**Funding/support:** This work was supported by the National Science Foundation of China (61420106001, 91420302, 61375111, 81271389, and 81471251); the National Basic Research Program of China (2013CB329401); and the Natural Science Foundation of Guangdong Province, China (grant no. S2013010014545).

The authors have no conflicts of interest to disclose.

<sup>a</sup> College of Mechatronics and Automation, National University of Defense Technology, Changsha, Hunan, <sup>b</sup> Department of Radiology, First Affiliated Hospital, Guangzhou University of Chinese Medicine, Guangzhou, Guangdong, China.

\* Correspondence: Prof Dewen Hu, College of Mechatronics and Automation, National University of Defense Technology, Changsha, Hunan 410073, China (e-mail: dwhu@nudt.edu.cn); Prof Shijun Qiu, Department of Radiology, First Affiliated Hospital, Guangzhou University of Chinese Medicine, Guangzhou, Guangdong 510405, China (e-mail: qiu-sj@163.com)

Copyright © 2016 the Author(s). Published by Wolters Kluwer Health, Inc. All rights reserved.

This is an open access article distributed under the terms of the Creative Commons Attribution-Non Commercial-No Derivatives License 4.0 (CCBY-NC-ND), where it is permissible to download and share the work provided it is properly cited. The work cannot be changed in any way or used commercially.

Medicine (2016) 95:29(e4275)

Received: 3 March 2016 / Received in final form: 11 June 2016 / Accepted: 23 June 2016

<http://dx.doi.org/10.1097/MD.0000000000004275>

## 1. Introduction

Nasopharyngeal carcinoma (NPC), the malignant tumors located in the nasopharynx, strongly affects patients' quality of lives with a high incidence rate in southern China.<sup>[1,2]</sup> Radiotherapy (RT) is one of the most fundamental treatment approaches for controlling and shrinking tumor due to the tumor's radiosensitive characteristic.<sup>[1,3]</sup> However, accompanying with the inhibition of the tumor, the irradiation also causes brain structural and functional injuries of some normal brain regions due to 2 reasons. First, brain regions such as the cerebellum, brain stem, inferior and medial temporal lobes<sup>[4,5]</sup> are very close to the tumor tissue, which are inevitably included in the target volume of irradiation. Second, to achieve good treatment efficacy, RT has to adopt an enough high dose of irradiation, which always exceeds the dose tolerance limit of normal brain regions.

Except for the brain structural abnormalities,<sup>[6]</sup> the radiation-induced functional deficits of NPC patients were also extensively investigated applying statistic analysis, such as performing the Montreal Cognitive Assessment (MoCA). Surveys have indicated that the NPC patients with RT (RT+) generally showed lower MoCA scores than the NPC patients without RT (RT-), demonstrating that RT would induce the cognitive deficits in NPC patients.<sup>[7]</sup> The radiation-induced functional impairments included the domains of short-term memory, language ability,

**Table 1****Characteristics of the participants in this study.**

Variable	Mean $\pm$ SD (range)		P
	RT– NPC	RT+ NPC	
Sample size	24	35	
Gender, male/female	15/9	28/7	0.14*
Age, y	39.13 $\pm$ 10.41 (21–53)	42.09 $\pm$ 8.44 (20–55)	0.23†
Education, y	10.96 $\pm$ 2.34	10.83 $\pm$ 2.16	0.83†
Postirradiation time, mo		18.14 $\pm$ 15.15 (6–87)	
Montreal Cognitive Assessment	27.29 $\pm$ 1.04 (25–29)	24.2 $\pm$ 1.35 (22–27)	2.7e – 13†

RT– NPC = NPC patients not receiving radiotherapy, RT+ NPC = NPC patients receiving radiotherapy, SD = standard deviation.

\* Pearson chi-square test.

† Two-sample *t* test.

list-generating fluency,<sup>[8]</sup> attention,<sup>[9]</sup> visual memory function,<sup>[10]</sup> and also motor abilities.<sup>[9]</sup>

However, to the best of our knowledge, there is no much investigation of radiation-induced functional brain alterations in NPC patients using functional magnetic resonance imaging (fMRI). The functional connectivity, which is built based on the fMRI data, is now vastly employed in investigating brain functions via showing the brain synchronized neural activity. The benefits of exploring the functional connectivity include 2 aspects. First, the functional connectivity changes reveal potential biomarkers, which would shed new light on the brain functional impairments.<sup>[11]</sup> Second, the functional connectivity alterations may provide valuable training and practice targets for further functional recovery treatments, considering the plastic characteristic of functional connectivity.<sup>[12,13]</sup>

Recently, multivariate pattern analysis (MVPA) techniques, especially support vector machine (SVM), have been effectively used in detecting the functional connectivity alterations in some psychiatric diseases.<sup>[14–17]</sup> SVM successfully recognizes a distinct pattern in identifying 2 groups with the maximum boundaries.<sup>[18]</sup> In our study, however, we use SVM to identify RT+ from RT– group not just concerning about the classification result, but more importantly about finding the reliable altered functional connectivity between these 2 groups. The main purpose is to explore the potential biomarkers of the radiation-induced functional impairments, while the classification results can be used as the indicator to show whether the features are representative enough in revealing the differences between these 2 groups.

Hence, the aim of our study is to evaluate the radiation-induced functional changes of NPC patients by examining the functional connectivity of RT– NPC and RT+ NPC patients, using SVM method. We focus only on the late delayed injury, which is considered to be exhibited more than 6 months later after receiving RT.<sup>[19]</sup> The MoCA was also applied to investigate the global cognitive performance of both RT+ and RT– patients.

Previous studies have reported the RT-induced brain structural and functional alterations in specific regions such as the cerebellum and the temporal lobe. However, the abnormality of a single brain region may induce the reorganization of the whole brain functional connectivity network, since the brain is a delicate system that utilizes multiple brain regions to execute complex cognitive tasks. Besides, the functional connectivity is demonstrated to be underlying the human behavior and cognitive functions.<sup>[20]</sup> Thus, we speculate that RT may alter the whole brain functional connectivity of NPC patients and these alterations may be relevant to the highly reported functional

impairments, such as attention, visual processing, and other cognitive functions.

## 2. Materials and methods

### 2.1. Participants

From April 2013 to February 2014, 59 nonkeratinizing undifferentiated NPC patients (with staging from T1N0M0 to T4N2M0, the 6th edition of the UICC/AJCC staging system for NPC) who had been diagnosed by nasopharyngeal biopsy and histopathology were brought into this study, including 24 patients who were just diagnosed with NPC and 35 RT+ patients who had also undergone chemotherapy. These 2 groups were matched in age, gender, education level, and clinic stage (Table 1). All subjects were right-handed, native Chinese speakers. In our study, the time interval between the completion of RT and the acquisition of the brain data in RT+ NPC group patients ranged from 6 to 87 months. All RT+ NPC patients received radical intensity-modulated radiation therapy using corvus system (Peacock, Nomos, Deer Park, IL), with a fixed mask after CT-Sim. They were irradiated with a linear accelerator (Varian 2300EX, Varian Medical Systems, Palo Alto, CA, USA) (Precision X-ray) for 6 to 7 weeks, which were divided into 30 to 33 fractions (once a day, quintic a week). The total dose of nasopharynx (gross tumor volume 1 [GTV1]) were 58 to 70 Gy, GTVnd were 54 to 64 Gy, and clinic target volume were 50 to 54 Gy. The dose-volume statistics for temporal lobes and brainstem were calculated (Table 2). In addition, according to the institutional guidelines, all RT+ NPC patients received neoadjuvant/adjuvant chemotherapy for 1 to 3 months before or after RT with 1 to 3 agents, such as cisplatin, 5-FU paclitaxel and docetaxel. The concurrent chemotherapy was conducted in 1 to 4 courses.

For patients who had intracranial invasion, brain tumor or metastases, brain trauma, leukoencephalopathy, alcoholism, hypertension, diabetes, neurologic or psychiatric diseases, and whose ages were lower than 18 years or more than 55 years were

**Table 2**

### Dose-volume statistics of organs at risk for 35 patients with nasopharyngeal carcinoma treated with intensity-modulated radiation therapy (Gy).

Organs at risk	Mean dose	Maximum dose	Minimum dose
Left temporal lobe	9.2–33.3 (18.2)	45.8–74.0 (65.2)	1.1–5.4 (2.7)
Right temporal lobe	7.9–32.5 (19.2)	50.9–71.6 (68.5)	1.1–6.5 (2.9)
Brainstem	16.4–40.2 (28.9)	24.7–78.5 (53.3)	1.9–21.0 (11.5)

excluded from this study. Each NPC patient's overall function was evaluated by using the Karnofsky performance status (KPS) scale. All subjects had a KPS score of  $\geq 80$ , indicating a high overall function. In addition, all subjects received the Beijing Version of MoCA by a neurological physician who was blinded to this study. Ethical approval was obtained from the Ethics Committee of Southern Medical University, and all participants provided written informed consent.

## 2.2. MRI acquisitions

All resting-state MRI data were acquired using a Philips Achieva 3.0T scanner (Philips Medical Systems, Best, Netherlands) with an 8-channel head coil for all the participants. Routine sequences including axial T1WI, T2WI, and fluid-attenuated inversion recovery images for every patient were acquired to detect any macroscopic lesion. The fMRI data were conducted using a gradient echo–echo planar imaging sequence covering the whole brain, which was paralleled to anterior-commissure–posterior-commissure plane. The scan parameters were performed as following: repetition time=2000 ms, echo time=30 ms, flip angle=90°, field of view=230 mm  $\times$  230 mm, matrix=128  $\times$  128, slice thickness=3 mm, with 1-mm gap, and total volumes=205. None of the subjects exhibited excessive head motions during the data acquisition ( $<2.5$ -mm translation in  $x$ -,  $y$ -, or  $z$ -axis and  $<1^\circ$  of rotation in each axis).

## 2.3. Data preprocessing

Standard preprocessing of the acquired functional images was conducted using the SPM8 package (Wellcome Department of Cognitive Neurology, Institute of Neurology, London, UK, <http://www.fil.ion.ucl.ac.uk/spm>). For each subject, we discarded the first 10 volumes to allow for magnetization equilibrium. The remaining 195 volumes were realigned to correct for the head motion and spatial normalized into the Montreal Neurological Institute template with a voxel size of  $3 \times 3 \times 3$ . After that the normalized volumes were spatial smoothed with a Gaussian smoothing kernel of 6 mm full-width at a half maximum. We further removed the linear trends of the volumes and temporal filtered the volumes with a Chebyshev band-pass filter (0.01–0.1 Hz). Finally, the filtered volumes were regressed out with altogether 9 coefficients, including the global mean, the confounding effects of cerebrospinal fluid and white matter, and the 6 head motion parameters.

## 2.4. Functional connectivity topography

To extract the whole brain functional connectivity, we selected 160 seed regions based on a recent fMRI study, which defined 6 brain networks and extracted 160 seed regions according to several functional tasks.<sup>[21]</sup> The time courses of the 160 seed regions with a spherical radius of 3 mm were extracted and Pearson correlation coefficients were calculated between each pairs of these 160 time series, which resulted in a  $160 \times 160$  functional connectivity matrix for each subject. Removing the diagonal elements and the symmetrical half, the remaining amount of functional connectivity elements was  $(160 \times 159)/2 = 12,720$ .

## 2.5. MVPA classification and leave-one-out cross-validation

We performed a soft-margin SVM analysis with the linear kernel and the regularization parameter  $C=1$ . Leave-one-out

cross-validation (LOOCV) was used to evaluate the general classification performance, while 1 test sample was leaving out by turns in each round of LOOCV, and all other samples were considered as training samples. Two-sample  $t$  test was used to test whether each of the 12,720 features was significantly different between the 2 groups of training samples. All 12,720 features were ranked according to their significance statics. The top-ranked  $K$  features were then selected in both the training set and testing set. The number of selected features  $K$  ranged from 50 to 5000. After that, locally linear embedding was used to reduce the feature dimension in the training samples, while the same projective matrix of dimension reduction was also applied in the testing sample to obtain the new testing features. An SVM classifier was then trained by the generated features in the training set and was applied to classify the testing sample. After all 59 rounds of LOOCV process, the general classification accuracy was obtained by calculating the proportion of testing samples that were correctly identified. Permutation test was performed for the classifier 10,000 times to empirically evaluate whether the classification accuracies were significantly greater than chance. The flowchart of the MVPA method was shown in Fig. 1.

## 2.6. Consensus functional connections

In each round, we measured the discriminative ability of each feature by ranking its absolute value of the  $T$  score in the two-sample  $t$  test. There were 59 LOOCV rounds and we considered 1 feature as a consensus feature if it was ranked within the top 200 features for more than half of these 59 rounds, which was set to 30 rounds finally.

## 2.7. MoCA measurement and correlation analysis

The MoCA was performed in measuring the cognitive performance of each NPC patient, in both RT+ and RT– groups. The MoCA score was the sum of 7 subitems, including visuospatial, executive, naming, memory, attention, language, abstraction, and orientation. We tested the linear correlation levels between the MoCA scores and the consensus functional connections, and between the 7 subscores and the consensus functional connections, respectively.

## 3. Results

### 3.1. Classification results

The SVM classifier effectively captured the different functional connectivity pattern between RT– and RT+ NPC patients. The most discriminating features were found, and the classifier achieved an overall accuracy of 81.36% in identifying the RT+ group from the RT– group (75% in RT– NPC and 85.71% in RT+ NPC), with 99.94% classification accuracy in training set. The statistic value of permutation test was  $P < 0.00001$ , which rejected the null hypothesis that the RT+ and RT– groups were subjected to the same distribution. This demonstrated that the classifier trained in our study learned the relationship between the data and the labels with a low probability of being wrong and the classification accuracies obtained in our study was statistically significant.

### 3.2. Consensus features

In this study, 45 functional connections were identified as the consensus features in the cross-validation (Table 3). Figure 2 showed the spatial locations of the 45 consensus functional

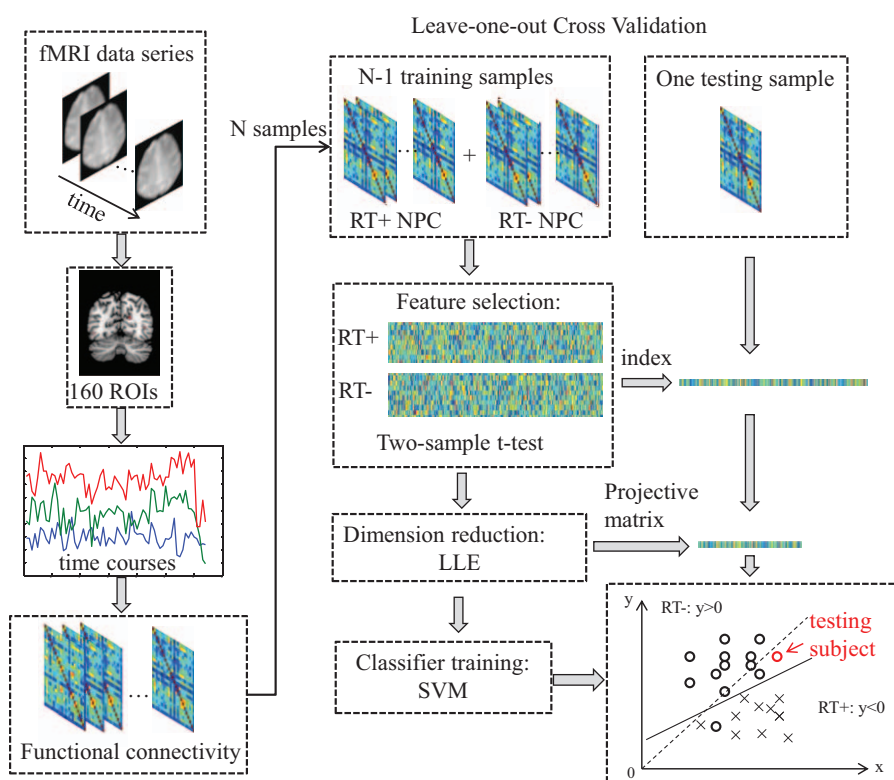


**Figure 1.** The workflow of the classification with leave-one-out evaluation in our study. ROI = regions of interest, LLE = locally linear embedding.

connections. The 6 networks were shown in 6 different colors. The size of each regions of interest was proportional to how many consensus features it participated in. Twenty-four functional connections of RT+ NPC were increased while 21 were decreased, comparing to RT- NPC. In Fig. 2, the orange and light blue lines indicated the increased and decreased functional connections, respectively. We found that the consensus features mainly located in the mutual connections between the networks of the cerebellum, cingulo-opercular, and sensorimotor.

### 3.3. Correlation analysis

The MoCA scores of RT+ NPC patients were significantly lower than RT- group with the significant level of  $P < 2.70e-13$  (Fig. 3). Five consensus connections were notably correlated with the MoCA overall scores, which were the functional connectivity between the vermis and hippocampus lobe ( $P < 0.00043$ ), cerebellum lobule VI and dorsolateral prefrontal cortex (dlPFC) ( $P < 0.00059$ ), precuneus and dorsal frontal cortex (dFC) ( $P < 0.00023$ ), cuneus and middle occipital lobe ( $P < 0.00071$ ), and anterior insula and cuneus ( $P < 0.00028$ ) (Fig. 4A–E). The significance coefficients were all false discovery rate corrected with the correction level of  $q < 0.05$ . Besides, after examined the correlation between all 7 subscores with the 45 consensus features, respectively, only 1 pair was found significantly correlated, which was the attention score and the functional connectivity between the vermis and hippocampus ( $P < 0.00072$ , uncorrected) (Fig. 4F).

## 4. Discussion

Our results demonstrated the radiation-induced brain functional connectivity abnormalities of NPC patients. The captured deficit

pattern of functional connectivity was reliable in identifying the RT- from RT+ with 81.36% accuracy. The 45 consensus connections were mainly the mutual connections between the cerebellum, sensorimotor, and cingulo-opercular networks. In addition, 5 consensus functional connections were significantly correlated with the MoCA scores, among which 1 connection was significantly correlated to the attention score. Together, these findings suggested that the altered functional connectivity pattern might serve as a potential biomarker of the radiation-induced brain dysfunctions in NPC patients.

The 45 consensus connections were associated with all of the 6 networks previously defined,<sup>[21]</sup> especially the mutual connections between the cerebellum, sensorimotor, and cingulo-opercular networks. The cerebellum is close to the tumor proximity, which is inevitably included in the radiation volume target, suffering a high irradiation dose.<sup>[22]</sup> Anatomical surveys indicated that the cerebellum is extensively interconnected with the cerebral cortex via thalamus in the output circuit, and via the pons in the input circuit, which forms a contralateral circuit.<sup>[23]</sup> Besides, it was demonstrated that the cerebellum is not only associated with motor control function, as traditionally considered, but is also involved in cognitive function.<sup>[24]</sup> In our exploration, though we chose the patients with normal appearing white matter and gray matter in the brain, the cerebellum was still strongly involved in the abnormal functional connectivity pattern. We speculated that the cerebellum function may be altered during the RT process in the RT+ NPC patients comparing to the RT- group, and the cerebellar-cerebral circuits may be damaged.

Our results found that the cerebellum network was abnormally connected with sensorimotor and cingulo-opercular network. The sensorimotor network is the coupling of sensory and motor functions, and the cingulo-opercular functional network is

**Table 3**

**Information on 45 consensus features. The positive feature weights mean that RT– NPC patients have larger feature values than RT+ group, while the negative feature weights mean RT– NPC patients have smaller feature values than RT+ group. The z-transformed correlation coefficients (Zcc) of RT– and RT+ NPC groups are included.**

Consensus features					Zcc	
Network1	Seed1	Network2	Seed2	Weight	RT–	RT+
Cerebellum	L_lat_cerebellum	Sensorimotor	L_temporal	5.244	0.17522	–0.05189
Default	R_vIPFC	Occipital	R_occipital	–4.367	–0.12724	0.05243
Cerebellum	R_med_cerebellum	Cingulo-opercular	L_post_insula	4.365	0.08326	–0.09615
Cerebellum	L_lat_cerebellum	Frontal-parietal	R_dIPFC	–4.269	–0.11313	0.09387
Default	R_sup_frontal	Sensorimotor	L_mid_insula	–4.240	–0.17714	0.01352
Default	R_precuneus	Frontal-parietal	R_dFC	4.172	0.12909	–0.07690
Frontal-parietal	R_vIPFC	Sensorimotor	R_parietal	–4.107	–0.07621	0.14067
Cerebellum	L_lat_cerebellum	Frontal-parietal	R_dIPFC	–4.070	–0.14380	0.03796
Cingulo-opercular	L_TPJ	Occipital	L_occipital	4.061	0.32311	0.07232
Cerebellum	L_lat_cerebellum	Cingulo-opercular	L_ACC	–3.967	–0.20786	–0.04496
Occipital	R_post_occipital	Sensorimotor	R_temporal	3.932	0.07161	–0.15990
Sensorimotor	SMA	Sensorimotor	R_temporal	3.887	0.05037	–0.16708
Cerebellum	L_inf_cerebellum	Occipital	R_post_occipital	–3.841	–0.14854	0.10987
Frontal-parietal	R_vIPFC	Occipital	R_occipital	–3.728	–0.18295	0.01708
Cerebellum	L_inf_cerebellum	Cingulo-opercular	R_inf_cerebellum	–3.716	–0.18155	0.08336
Default	L_occipital	Occipital	R_occipital	3.668	0.25202	0.02350
Frontal-parietal	R_vIPFC	Occipital	R_temporal	–3.653	–0.17477	0.02140
Frontal-parietal	R_dFC	Sensorimotor	R_parietal	–3.629	0.05515	0.25867
Default	L_occipital	Sensorimotor	R_parietal	3.607	0.09102	–0.07487
Cingulo-opercular	R_parietal	Cingulo-opercular	R_temporal	3.606	0.18880	0.00541
Cerebellum	L_lat_cerebellum	Sensorimotor	R_precentral_gyrus	–3.598	–0.23424	–0.08990
Cingulo-opercular	R_ant_PFC	Cingulo-opercular	R_ant_insula	3.572	0.28408	0.07370
Cingulo-opercular	R_temporal	Default	L_ant_PFC	–3.560	–0.16841	–0.00038
Cingulo-opercular	L_vFC	Sensorimotor	R_parietal	–3.543	–0.16728	0.04548
Cerebellum	L_lat_cerebellum	Cingulo-opercular	L_post_cingulate	3.533	0.17039	0.02186
Occipital	R_post_occipital	Sensorimotor	R_frontal	3.512	0.07842	–0.13197
Cerebellum	R_med_cerebellum	Cingulo-opercular	R_aPFC	–3.509	–0.16891	0.02767
Cerebellum	L_lat_cerebellum	Default	R_precuneus	3.508	0.07414	–0.07202
Occipital	L_occipital	occipital	R_occipital	3.502	0.14859	–0.04454
Cingulo-opercular	L_temporal	Frontal-parietal	L_vent_aPFC	–3.492	0.16599	0.36572
Frontal-parietal	L_ACC	Sensorimotor	R_temporal	3.486	0.01906	–0.17795
Cingulo-opercular	R_basal_ganglia	Sensorimotor	R_vFC	3.484	0.26944	0.03535
Cingulo-opercular	L_ant_insula	Sensorimotor	R_parietal	–3.481	–0.20973	–0.02838
Cingulo-opercular	R_basal_ganglia	Sensorimotor	R_precentral_gyrus	3.465	0.20700	0.00911
Cingulo-opercular	L_post_cingulate	Frontal-parietal	L_dIPFC	–3.447	–0.08466	0.07173
Cerebellum	L_lat_cerebellum	Default	L_post_cingulate	3.424	0.17139	–0.00480
Cerebellum	R_lat_cerebellum	Sensorimotor	R_vFC	–3.424	–0.13902	0.04034
Cerebellum	L_lat_cerebellum	Default	L_precuneus	3.410	0.06916	–0.06504
Cerebellum	L_inf_cerebellum	Cingulo-opercular	R_fusiform	–3.401	–0.31431	–0.04993
Default	L_occipital	Frontal-parietal	R_dFC	3.390	0.01624	–0.15422
Cerebellum	L_lat_cerebellum	Sensorimotor	R_frontal	–3.385	–0.16324	0.02691
Sensorimotor	L_mid_insula	Sensorimotor	R_parietal	–3.381	–0.13252	0.04859
Cingulo-opercular	L_post_cingulate	Sensorimotor	R_frontal	–3.376	–0.13785	0.01461
Cerebellum	L_lat_cerebellum	Occipital	L_occipital	3.374	0.01950	–0.13097
Cingulo-opercular	L_ant_insula	Occipital	R_occipital	–3.370	–0.16121	–0.00005

ACC = anterior cingulate cortex, ant = anterior, dFC = dorsal frontal cortex, dIPFC = dorsolateral prefrontal cortex, dPC = dorsal prefrontal cortex, inf = inferior, L = left, lat = lateral, med = median, mid = middle, PFC = prefrontal cortex, aPFC = anterior prefrontal cortex, post = posterior, R = right, SMA = supplemental motor area, sup = superior, TPJ = temporoparietal junction, vent = ventral, vFC = ventral prefrontal cortex, vIPFC = ventrolateral prefrontal cortex.

associated with controlling goal-directed behaviors.<sup>[25]</sup> We proposed that the functional connectivity alterations between the cerebellum and sensorimotor network might imply the radiation-induced motor deficits in NPC patients, while the functional connectivity alterations between the cerebellum and cingulo-opercular network may involve in the cognitive functional abnormalities. Indeed, the motor ability deficit was previously demonstrated in the NPC RT+ patient.<sup>[26]</sup> In some clinical reports, the RT+ NPC patients exhibited swallowing impairment and bulbar palsy,<sup>[27]</sup> which were involved in the sensorimotor function deficits.

The correlation analysis showed that 5 consensus functional connections were significantly correlated with the MoCA scores, which included the functional connections between the vermis and hippocampus, cerebellum lobule VI and dIPFC, precuneus and dorsal frontal lobe, cuneus and middle occipital lobe, and insula and cuneus.

Hippocampus plays an important role in the information consolidation and spatial navigation, and is also known to be involved in attention processes such as visuospatial working memory<sup>[28]</sup> and modulating executive functions.<sup>[29]</sup> Studies have reported that the RT would induce the hippocampus structural

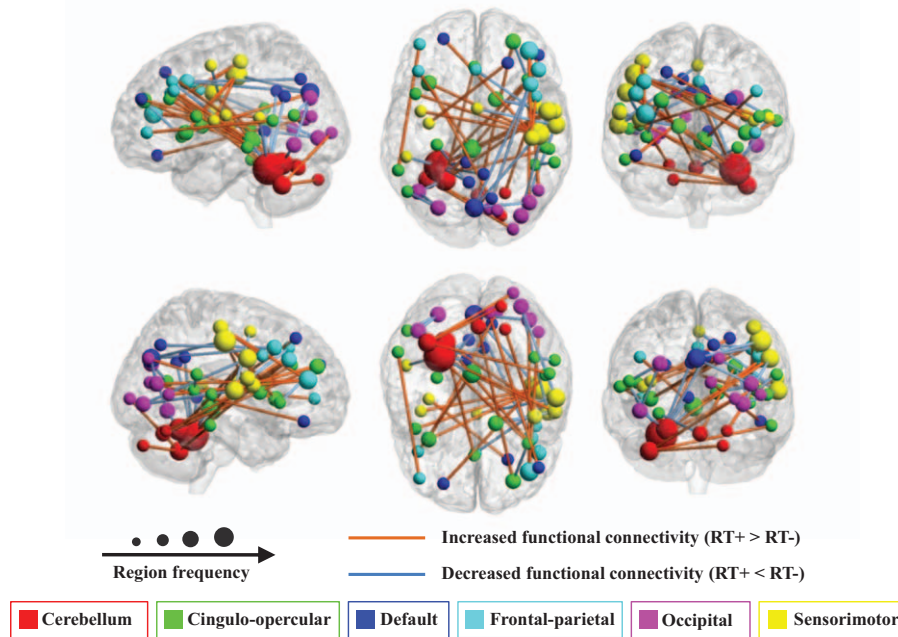


**Figure 2.** The regional weights and distribution of the 45 consensus functional connections. Regions are color-coded by 6 brain networks.<sup>[21]</sup> The size of the regions is proportional to the frequency of the region in these functional connections. The lines between regions indicate the functional connectivity. Yellow lines means the functional connectivity of RT+ NPC is increased comparing to RT– NPC, while the light blue line means decreased functional connectivity. This figure shows that the majority of the consensus features locate in the mutual connectivity between 3 networks: the cerebellum, the cingulo-opercular, and the sensorimotor networks.

deficit.<sup>[30]</sup> Recently, a study using clustering method to identify brain networks demonstrated an important role of vermis in the ventral attention network.<sup>[31]</sup> Indeed, both the hippocampus<sup>[32]</sup> and vermis<sup>[33]</sup> were found abnormal in the attention deficit hyperactivity disorder (ADHD), a disease that always has a high level of impulsivity and inattentiveness.<sup>[34]</sup> In our study, we found that the functional connectivity between the vermis and hippocampus was significantly correlated with the MoCA scores, especially with the attention score. These results suggested that the altered functional connectivity between the vermis and hippocampus might imply the attention deficit in RT+ NPC patients.

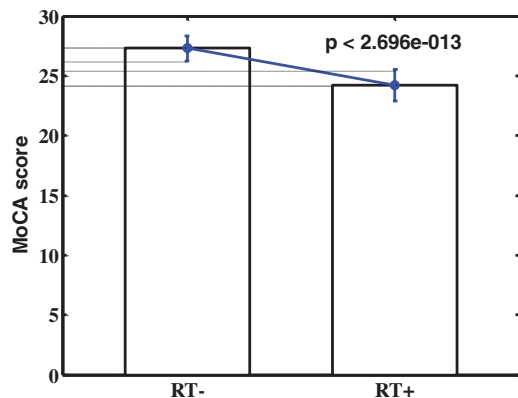


**Figure 3.** The statistic comparison between the MoCA scores of RT– and RT+ NPC patients. This figure shows that the MoCA score of NPC patients is significantly decreased after receiving RT with the significance level of  $P < 2.696e - 013$ .

The cuneus is involved in the visual processing,<sup>[35]</sup> while the middle occipital lobe is also considered as an important visual processing region. The altered functional connectivity between the cuneus and middle occipital lobe may suggest that RT process would induce the visual processing deficits in the NPC patients. Indeed, studies have reported the altered visual memory in RT+ NPC patients.<sup>[36]</sup> Apart from the traditional visual function, cuneus is recently demonstrated to be involved in the inhibition control.<sup>[37]</sup> Besides, the anterior insula is engaged in higher order awareness and cognitive processing.<sup>[38]</sup> We suggested that the altered functional connectivity between cuneus and insula might reveal the impaired cognitive control in NPC patients with RT. Moreover, the precuneus involves in the self-related awareness<sup>[39]</sup> and conscious information processing,<sup>[40]</sup> while the dlPFC and dFC are related to executive processing<sup>[41]</sup> and social cognition.<sup>[42]</sup> Except for the traditional sensorimotor function, the lobule VI takes part in cognitive and emotional processing, and also in the prefrontal–cerebellar loops of executive functions.<sup>[23]</sup> The altered functional connectivity between the precuneus and dFC, and also between the lobule VI and dlPFC may reveal the impaired cognitive and executive processing.<sup>[43]</sup>

The altered functional connectivity pattern and the significant correlations between 5 altered connections and MoCA scores demonstrated that RT may induce the brain cognitive dysfunctions, especially attention alterations. This indicates that radiation-induced brain impairments are not restricted to the exposed area, other encephalic region, such as cerebellum, sensorimotor, and cingulo-opercular areas, should be concerned as well.

Our study showed that RT would cause brain functional connectivity abnormalities in NPC patients. The 45 altered functional connections may serve as the potential biomarkers and may underlie the RT-induced functional impairments. Hence, the

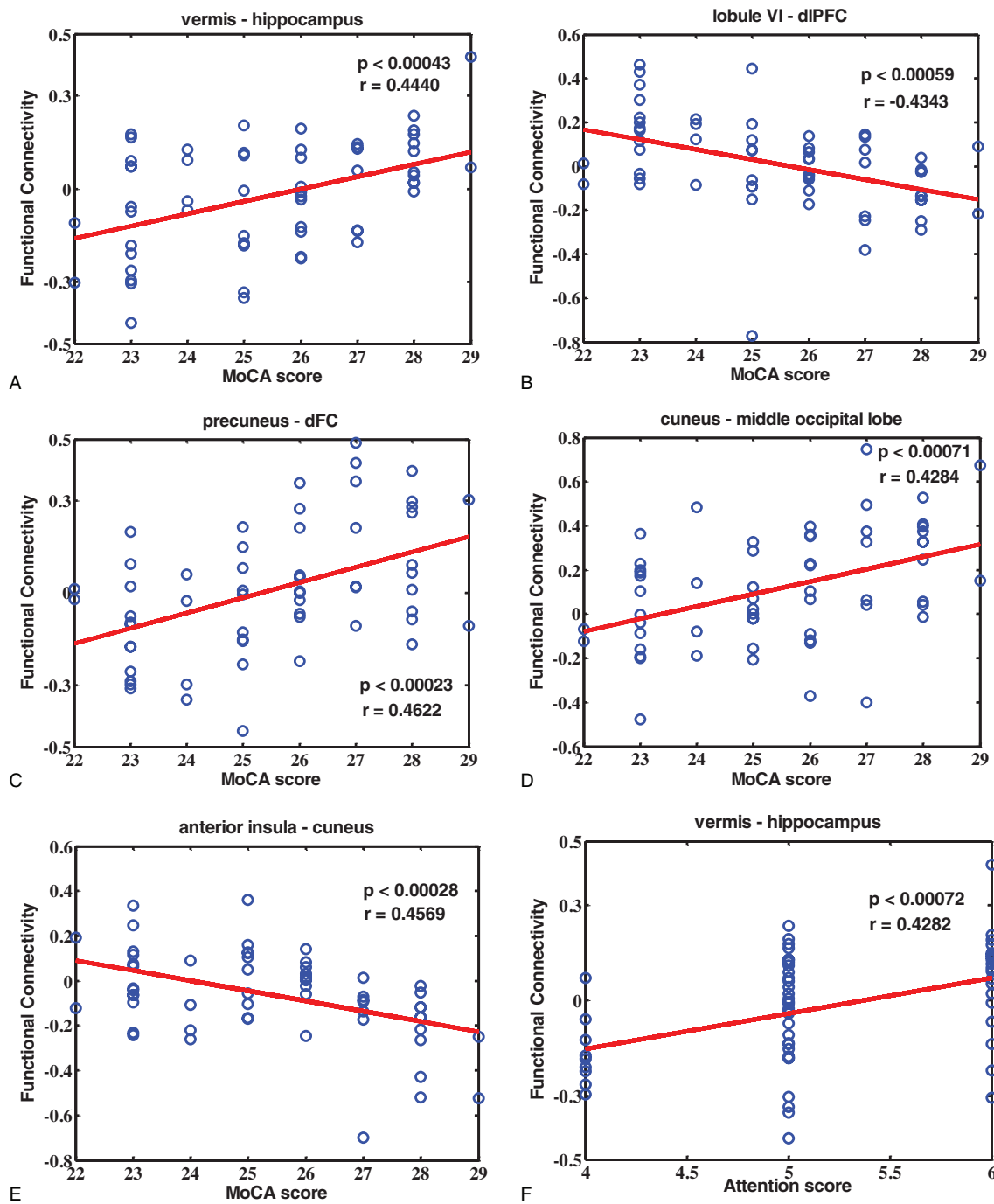


**Figure 4.** Correlation rates and significant levels between the consensus features and MoCA scores, as well as attention score. (A) The functional connectivity between vermis and hippocampus is positively correlated with MoCA score ( $P=0.00043$ ,  $r=0.4440$ ; FDR corrected,  $q < 0.05$ ); (B) the functional connectivity between cerebellum lobule VI and dlPFC is negatively correlated with MoCA score ( $P=0.00059$ ,  $r=-0.4343$ ; FDR corrected,  $q < 0.05$ ); (C) the functional connectivity between precuneus and dFC is positively correlated with MoCA score ( $P=0.00023$ ,  $r=0.4622$ ; FDR corrected,  $q < 0.05$ ); (D) the functional connectivity between cuneus and middle occipital lobe is positively correlated with MoCA score ( $P=0.00071$ ,  $r=0.4284$ ; FDR corrected,  $q < 0.05$ ); (E) the functional connectivity between anterior insula and cuneus is negatively correlated with MoCA score ( $P=0.00028$ ,  $r=0.4569$ ; FDR corrected,  $q < 0.05$ ); and (F) the functional connectivity between vermis and hippocampus is positively correlated with attention score ( $P=0.00072$ ,  $r=0.4282$ ; uncorrected). dlPFC = dorsolateral prefrontal cortex, dFC = dorsal frontal cortex.

potential clinical value and application of our study may exist in 3 aspects. First, we suggest that to prevent the RT-induced cognitive impairments as much as possible, some necessary measures may be taken for the conventional MRI negative NPC patients, such as using hyperbaric oxygen therapy and radio-protector, like glucocorticoid, melatonin, magnesium sulfate,

valproate, and cyclooxygenase inhibitors. Second, it is important for radiation oncologists to evaluate the cognitive deficits in NPC patients after the RT process. In our study, we found that RT may induce various functional impairment including domains of attention, visual processing, inhibition control, and executive processing. Based on these, some of the clinical interventions

relative to these cognitive deficits shall be considered as a further follow-up recovery treatment. For example, the attention dysfunction and inhibition control deficit, which are coincident with ADHD, are clinically treated in 2 ways, including the pharmacological treatment such as applying stimulants and atomoxetine, and also the recommended nonpharmacological interventions such as neurofeedback, cognitive training, and restricted elimination diets.<sup>[44]</sup> These widely used treatments may also help to decrease the RT-induced attention alterations in NPC patients. Last but not the least, recent studies have investigated some promising method such as brain stimulation, which aims to regulate the altered functional connectivity and reduce the brain functional impairments.<sup>[12,13]</sup> Thus, the 45 altered functional connections found in our study not only underlie the pathology of the RT-induced functional impairments but may also serve as the stimulating targets, which might to some extent help the RT+ NPC patients recover from the functional impairments.

In our study, apart from RT, the chemotherapy might also cause the functional connectivity alterations in RT+ NPC patients, since the RT- NPC patients did not receive RT or chemotherapy, while RT+ NPC patients received both treatments. Though there is no report on NPC patients, studies on breast cancer patients have demonstrated that chemotherapy would cause some functional connectivity changes, especially in the default mode network,<sup>[45-47]</sup> the connectivity relevant to anterior cingulate cortex<sup>[48]</sup> and intraparietal sulcus.<sup>[45]</sup> These functional connectivity alterations may be underlying the executive, attention impairments,<sup>[45,46]</sup> and memory difficulties.<sup>[47]</sup> It was worth noting that the fMRI data in our study were scanned at least 6 months after the completion of chemotherapy, which would to a large extent reduce the chemotherapy-induced influence. Studies have demonstrated that the chemotherapy-induced functional impairments would recover largely over time, particularly after 6 months, in breast cancer patients<sup>[49]</sup> or colon cancer patients.<sup>[50]</sup> Despite these, the potential functional connectivity alterations induced by chemotherapy in NPC patients remained unclear. Further study is needed in investigating the chemotherapy-induced functional connectivity alterations.

There are still some limitations in this study due to the small sample size and the lack of a new and larger sample to confirm the results of the classification performance and correlation analysis. In the future, we expect to collect a larger sample of follow-up NPC patients to evaluate the functional connectivity abnormalities, which can contribute to find more accurate and reliable functional connectivity pattern in revealing the RT-induced functional impairments.

## 5. Conclusion

The present study demonstrated that the whole brain functional connectivity pattern of RT+ NPC patients was significantly impaired comparing to RT- NPC group and the altered functional connectivity pattern was highly correlated with the MoCA score. These findings suggested that RT process might notably induce functional deficits in brain cognition, especially attention function. The 45 altered functional connections, especially the 5 connections that were significantly correlated to the MoCA scores, may shed new light on the underlying radiation-induced functional impairments in NPC patients and may serve as the potential indicators for further clinical recovery treatment of the impaired functions.

## References

- Chan AT. Nasopharyngeal carcinoma. *Ann Oncol* 2010;21(suppl 7):308-12.
- Jemal A, Bray F, Center MM, et al. Global cancer statistics. *CA Cancer J Clin* 2011;61:69-90.
- King AD, Ahuja AT, Yeung DK, et al. Delayed complications of radiotherapy treatment for nasopharyngeal carcinoma: imaging findings. *Clin Radiol* 2007;62:195-203.
- Brennan B. Nasopharyngeal carcinoma. *Orphanet J Rare Dis* 2006;1:23.
- Tsui EY, Chan JH, Ramsey RG, et al. Late temporal lobe necrosis in patients with nasopharyngeal carcinoma: evaluation with combined multi-section diffusion weighted and perfusion weighted MR imaging. *Eur J Radiol* 2001;39:133-8.
- Chen WS, Li JJ, Zhang JH, et al. Magnetic resonance spectroscopic imaging of brain injury after nasopharyngeal cancer radiation in early delayed reaction. *Genet Mol Res* 2014;13:6848-54.
- Wu X, Gu M, Zhou G, et al. Cognitive and neuropsychiatric impairment in cerebral radionecrosis patients after radiotherapy of nasopharyngeal carcinoma. *BMC Neurol* 2014;14:10.
- Hsiao KY, Yeh SA, Chang CC, et al. Cognitive function before and after intensity-modulated radiation therapy in patients with nasopharyngeal carcinoma: a prospective study. *Int J Radiat Oncol Biol Phys* 2010;77:722-6.
- Cheung M, Chan AS, Law SC, et al. Cognitive function of patients with nasopharyngeal carcinoma with and without temporal lobe radionecrosis. *Arch Neurol* 2000;57:1347-52.
- Lam LC, Leung SF, Chow LY. Functional experiential hallucinosis after radiotherapy for nasopharyngeal carcinoma. *J Neurol Neurosurg Psychiatry* 1998;64:259-61.
- Murphy K, Birn RM, Bandettini PA. Resting-state fMRI confounds and cleanup. *NeuroImage* 2013;80:349-59.
- Kelly C, Castellanos FX. Strengthening connections: functional connectivity and brain plasticity. *Neuropsychol Rev* 2014;24:63-76.
- Luft CD, Pereda E, Banissy MJ, et al. Best of both worlds: promise of combining brain stimulation and brain connectome. *Front Syst Neurosci* 2014;8:132.
- Mwangi B, Ebmeier KP, Matthews K, et al. Multi-centre diagnostic classification of individual structural neuroimaging scans from patients with major depressive disorder. *Brain* 2012;135(pt 5):1508-21.
- Shen H, Wang L, Liu Y, et al. Discriminative analysis of resting-state functional connectivity patterns of schizophrenia using low dimensional embedding of fMRI. *NeuroImage* 2010;49:3110-21.
- Liu F, Guo W, Fouche JP, et al. Multivariate classification of social anxiety disorder using whole brain functional connectivity. *Brain Struct Funct* 2015;220:101-15.
- Liu F, Xie B, Wang Y, et al. Characterization of post-traumatic stress disorder using resting-state fMRI with a multi-level parametric classification approach. *Brain Topogr* 2015;28:221-37.
- Vapnik VN. *The nature of statistical learning theory*. New York, NY: Springer-Verlag New York, Inc; 1995.
- Chan YL, Leung SF, King AD, et al. Late radiation injury to the temporal lobes: morphologic evaluation at MR imaging. *Radiology* 1999;213:800-7.
- Stevens WD, Spreng RN. Resting-state functional connectivity MRI reveals active processes central to cognition. *Wiley Interdiscip Rev Cogn Sci* 2014;5:233-45.
- Dosenbach NU, Nardos B, Cohen AL, et al. Prediction of individual brain maturity using fMRI. *Science* 2010;329:1358-61.
- Katoh N, Yasuda K, Shiga T, et al. A new brain positron emission tomography scanner with semiconductor detectors for target volume delineation and radiotherapy treatment planning in patients with nasopharyngeal carcinoma. *Int J Radiat Oncol Biol Phys* 2012;82:e671-6.
- Stoodley CJ, Schmahmann JD. Evidence for topographic organization in the cerebellum of motor control versus cognitive and affective processing. *Cortex* 2010;46:831-44.
- Buckner RL. The cerebellum and cognitive function: 25 years of insight from anatomy and neuroimaging. *Neuron* 2013;80:807-15.
- Dosenbach NU, Fair DA, Cohen AL, et al. A dual-networks architecture of top-down control. *Trends Cogn Sci* 2008;12:99-105.
- Cheung MC, Chan AS, Law SC, et al. Cognitive function of patients with nasopharyngeal carcinoma with and without temporal lobe radionecrosis. *Arch Neurol* 2000;57:1347-52.
- Chew NK, Sim BF, Tan CT, et al. Delayed post-irradiation bulbar palsy in nasopharyngeal carcinoma. *Neurology* 2001;57:529-31.

- [28] Bedard AC, Martinussen R, Ickowicz A, et al. Methylphenidate improves visual-spatial memory in children with attention-deficit/hyperactivity disorder. *J Am Acad Child Adolesc Psychiatry* 2004;43:260–8.
- [29] Sergeant JA, Geurts H, Oosterlaan J. How specific is a deficit of executive functioning for attention-deficit/hyperactivity disorder? *Behav Brain Res* 2002;130:3–28.
- [30] Greene-Schloesser D, Robbins ME, Peiffer AM, et al. Radiation-induced brain injury: a review. *Front Oncol* 2012;2:73.
- [31] Buckner RL, Krienen FM, Castellanos A, et al. The organization of the human cerebellum estimated by intrinsic functional connectivity. *J Neurophysiol* 2011;106:2322–45.
- [32] Perlov E, Philipsen A, van Elst TL, et al. Hippocampus and amygdala morphology in adults with attention-deficit hyperactivity disorder. *J Psychiatry Neurosci* 2008;33:509–15.
- [33] Glaser PE, Surgener SP, Grondin R, et al. Cerebellar neurotransmission in attention-deficit/hyperactivity disorder: does dopamine neurotransmission occur in the cerebellar vermis? *J Neurosci Methods* 2006;151:62–7.
- [34] DuPaul GJ. *ADHD rating scale-IV: checklists, norms, and clinical interpretation*. New York, NY:Guilford Press; 1998.
- [35] Hahn B, Ross TJ, Stein EA. Neuroanatomical dissociation between bottom-up and top-down processes of visuospatial selective attention. *NeuroImage* 2006;32:842–53.
- [36] Cheung MC, Chan AS, Law SC, et al. Impact of radionecrosis on cognitive dysfunction in patients after radiotherapy for nasopharyngeal carcinoma. *Cancer* 2003;97:2019–26.
- [37] Crockford DN, Goodyear B, Edwards J, et al. Cue-induced brain activity in pathological gamblers. *Biol Psychiatry* 2005;58:787–95.
- [38] Chikama M, McFarland NR, Amaral DG, et al. Insular cortical projections to functional regions of the striatum correlate with cortical cytoarchitectonic organization in the primate. *J Neurosci* 1997;17:9686–705.
- [39] Lou HC, Luber B, Crupain M, et al. Parietal cortex and representation of the mental self. *Proc Natl Acad Sci U S A* 2004;101:6827–32.
- [40] Vogt BA, Laureys S. Posterior cingulate, precuneal and retrosplenial cortices: cytology and components of the neural network correlates of consciousness. *Prog Brain Res* 2005;150:205–17.
- [41] Greene JD, Sommerville RB, Nystrom LE, et al. An fMRI investigation of emotional engagement in moral judgment. *Science* 2001;293:2105–8.
- [42] Miller BL, Cummings JL. *The human frontal lobes: functions and disorders*. New York, NY:Guilford Press; 2007.
- [43] Passamonti L, Novellino F, Cerasa A, et al. Altered cortical-cerebellar circuits during verbal working memory in essential tremor. *Brain* 2011;134(pt 8):2274–86.
- [44] Thapar A, Cooper M. Attention deficit hyperactivity disorder. *Lancet* 2016;387:1240–50.
- [45] Dumas JA, Makarewicz J, Schaubhut GJ, et al. Chemotherapy altered brain functional connectivity in women with breast cancer: a pilot study. *Brain Imaging Behav* 2013;7:524–32.
- [46] Hosseini SM, Kesler SR. Multivariate pattern analysis of fMRI in breast cancer survivors and healthy women. *J Int Neuropsychol Soc* 2014;20:391–401.
- [47] Kesler SR, Wefel JS, Hosseini SM, et al. Default mode network connectivity distinguishes chemotherapy-treated breast cancer survivors from controls. *Proc Natl Acad Sci U S A* 2013;110:11600–5.
- [48] Miao H, Li J, Hu S, et al. Long-term cognitive impairment of breast cancer patients after chemotherapy: a functional MRI study. *Eur J Radiol* 2016;85:1053–7.
- [49] Jansen CE, Cooper BA, Dodd MJ, et al. A prospective longitudinal study of chemotherapy-induced cognitive changes in breast cancer patients. *Support Care Cancer* 2011;19:1647–56.
- [50] Cruzado JA, Lopez-Santiago S, Martinez-Marin V, et al. Longitudinal study of cognitive dysfunctions induced by adjuvant chemotherapy in colon cancer patients. *Support Care Cancer* 2014;22:1815–23.